THE JOURNAL OF PHYSICAL CHEMISTRY B

Article

Elasticity-Based Patterning of Red Blood Cells on Undulated Lipid Membranes Supported on Porous Topographic Substrates

Sang-Wook Lee, Cherlhyun Jeong, and Sin-Doo Lee

J. Phys. Chem. B, **Article ASAP** • DOI: 10.1021/jp806753f • Publication Date (Web): 19 December 2008

Elasticity-Based Patterning of Red Blood Cells on Undulated Lipid Membranes Supported on Porous Topographic Substrates†

Sang-Wook Lee, Cherlhyun Jeong, and Sin-Doo Lee*

School of Electrical Engineering #032, Seoul National University, Kwanak P.O. Box 34, Seoul 151-600, South Korea

Received: July 30, 2008; Revised Manuscript Received: November 17, 2008

We describe elasticity-based patterning of human red blood cells (RBCs) into a microarray form on supported lipid membranes (SLMs) prepared on a solid substrate having two types of topographic patterns, porous and flat regions. The underlying concept is to precisely control the interplay between adhesion and the bending rigidity of the RBCs that interact with the SLMs. Attachment of the RBCs on highly undulated SLMs formed on the porous region is not energetically favorable, since membrane bending of the RBCs costs a high curvature elastic energy which exceeds adhesion. The RBCs are thus selectively confined within relatively flat regions of the SLMs without causing considerable elastic distortions. It was found that the population of the RBCs in a single corral is linearly proportional to the area of one element in our microarray.

Introduction

Recently, micropatterning of a variety of biological cells into a two-dimensional (2-D) array is of great interest in relation to fundamental studies of cellular activities, including cell adhesion,[1] migration,[2] and growth,[3] as well as practical applications for ultrasensitive cell-based biosensors,[4] programmed drug delivery,[5] and tissue engineering.[6] For precise cellular patterning, it is extremely important to generate spatially selective cell-adherent regions surrounded by a cell-repellent background.[7,8] In this regard, the patterning schemes of living cells have been dictated by surface modifications through microcontact printing,[9] photolithography,[10] or stencil-assisted patterning[11] that provides suitable biochemical functionalizations. For instance, extracellular matrix proteins[11] such as collagen and fibronectin are known to promote cell adhesion. In contrast, a poly(ethylene glycol)-modified self-assembled monolayer (SAM) of alkanethiols[12] on a gold substrate suppresses the protein adsorption and the subsequent cell adhesion. However, the existing surface modifications have such disadvantages that often limit the types of substrates, for example, gold films needed for the thiol-based SAM patterning.[12] Moreover, the availability of proper biochemical materials and the long-term stability of the physisorbed layer need to be considered.[13] One of the most important factors that govern patterning of various cells into a microarray is to construct such a biomimetic environment that prevents cells from denaturalization and contamination. The supported lipid membranes (SLMs), known as an *in vitro* model system for a biological membrane, represent a natural biofunctional surface serving as a platform for studying cellular activities such as adhesion and growth.

Here, we report on an elastic approach to patterning of human red blood cells (RBCs) into a microarray format on lipid membranes supported on a solid substrate having porous and flat topographies. The RBC has a well-defined biconcave structure. In addition, its chemical and physical properties such as the composition of lipids,[14] the membrane bending modulus,[15] and the adhesion force[16] are quite well-known. From the pathological viewpoint, the adhesion properties of the RBC would shed light on the generic features of malaria, diabetes, and sickle cell disease.[17] The SLM, a biomimetic surface which interacts with the plasma membrane of the RBC, was first prepared on the substrate with two different topographies. The RBCs were then selectively confined within the flat regions of the SLMs, since membrane bending of the RBCs on the highly undulated SLMs in the porous regions is not energetically favorable. Within the framework of de Gennes's elastic theory for layered structures of soft matter,[18] the elastic distortions of the SLMs as well as the plasma membranes of the RBCs on our topographic porous substrate were described in terms of the Helfrich-type energy.[19] It was found that the SLM on the porous topography provides a cell-repellent environment while that on the flat topography behaves as the cell-adhesive surface. The population of the RBCs in a single corral depends on the physical dimension of one element, being flat, in our array.

Figure 1 shows the schematic diagrams illustrating our topographic approach to the site-selective adhesion of the RBCs. The SLM was first formed from vesicles on a solid substrate having porous and flat topographies (Figure 1a). The RBCs were then deposited by gravitational sedimentation on the prepared SLM (Figure 1b). The adhesion of the RBCs in flat regions is relatively strong compared to the magnitude of the gravitational energy. Note that the RBCs in the porous regions were detached and moved into the buffer under the gravitational force when the substrate was held upside down (Figure 1c). The contact of the RBC with the SLM in the porous region and that in the flat region are shown in parts d and e of Figure 1, respectively. Considering that the bending rigidity of the plasma membrane of the RBC is sufficiently high (about 44 k_BT with the Boltzmann constant k_B and temperature T),[15] the RBC will not be considerably deformed and thus weak adhesion to the SLM is expected on the porous region. This results in easy detachment of the RBC from the porous region into buffer by the gravitational force.

† Part of the "PGG (Pierre-Gilles de Gennes) Memorial Issue".

* Corresponding author. E-mail: sidlee@plaza.snu.ac.kr. Phone:+82-2-880-1823. Fax: +82-2-874-9769.

10.1021/jp806753f CCC: $40.75

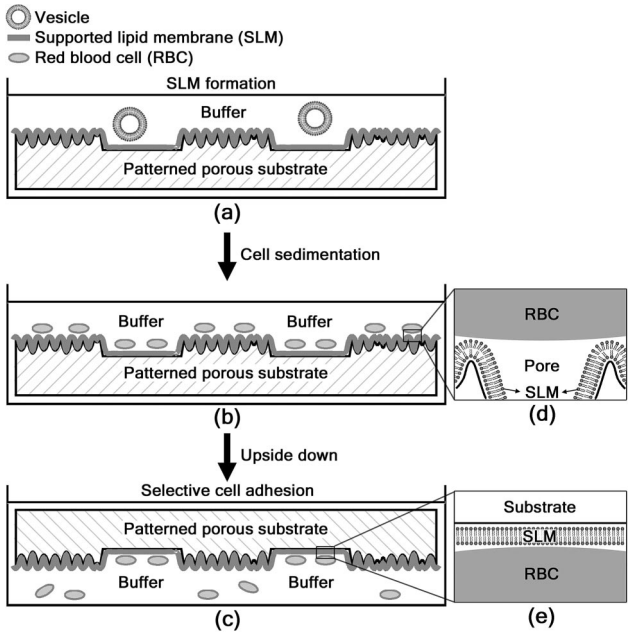

Figure 1. Schematic diagrams showing the underlying concept of the site-selective adhesion of the RBCs: (a) the formation of SLMs from vesicles; (b) cell sedimentation on SLMs; (c) selective adhesion of the RBCs in the flat regions against the gravitational force; (d) the contact of the RBC with the SLM on the top edge of the pore; (e) the contact of the RBC with the SLM in the flat region.

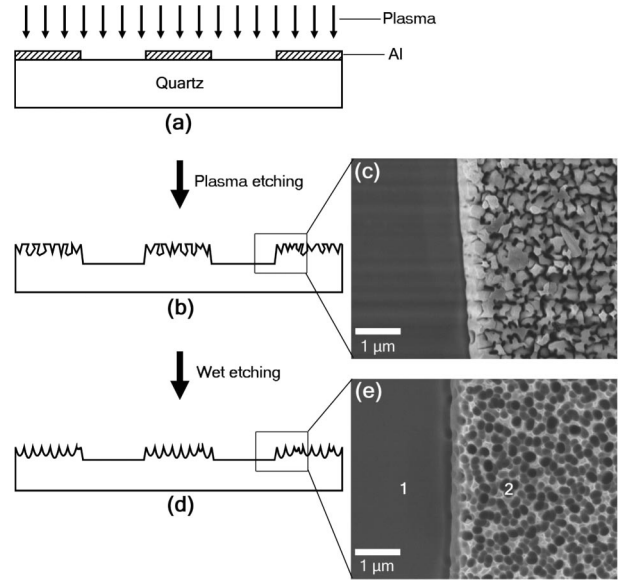

Figure 2. Fabrication of the porous and flat topographies on a quartz substrate: (a) plasma etching on the substrate surface with a patterned Al layer; (b) irregularly etched regions with Al and flat regions with no Al; (c) the SEM image of the flat and irregularly etched regions; (d) porous and flat topographies after chemical etching; (e) the SEM image of the flat (label 1) and porous topographies (label 2).

Experimental Section

1. Fabrication of Porous and Flat Topographies. Figure 2 shows the fabrication process of the porous and flat topographies on a quartz substrate used in this work. A thin aluminum (Al) layer of 100 nm thickness was first coated on a (100) quartz wafer and subsequently patterned by the conventional photolithography to define Al-covered and uncovered regions (Figure 2a). Using plasma etching equipment (AOE, STS, UK), plasma of C_4F_8 and O_2 was produced at a radio frequency of 13.56 MHz. During plasma etching for 6 min, the bare quartz regions were etched uniformly to be flat and the Al-covered regions were etched irregularly due to the Al clusters left in part (Figure 2b). Figure 2c shows an image of the etched substrate, observed with a scanning electron microscope (SEM; JSM-6700F, JEOL, Japan), where the boundary between a flat region and a plasma etched region can be seen. The porous topography used in our study, as shown in Figure 2d and e, was finally obtained by further chemically etching the plasma etched substrate with a buffer solution of HF (7:1 (v/v) NH_4F:HF) for 30 s. Note that the chemical etching process was carried out to remove any remaining Al on the substrate surface and to have pore surfaces be smooth.

2. Preparation the SLMs. The phospholipid used as a base for the formation of the SLMs was 1,2-dioleoyl-*sn*-glycero-3-phossphocholine (DOPC, Avanti Polar Lipids, Birmingham, AL). For imaging the SLMs, a red fluorescent dye-labeled lipid, 1,2-dihexadecanoyl-*sn*-glycero-3-phosphoethanolamine (Texas red-DHPE, Invitrogen, Eugene, OR) was mixed with DOPC at 1 mol %. The two components were dissolved in chloroform. The rapid solvent exchange method[20] involving evaporation of solvent, desiccation, and hydration processes was carried out at room temperature. The buffer contained 100 mM NaCl and 10 mM Tris at pH 8.0. The hydration was performed at a concentration of 0.2 mg/mL. Small unilamellar vesicles (SUVs) were obtained by the extrusion method (Mini-Extruder, Avanti Polar Lipid) with at least 20 filtering processes through a 50 nm filter. The substrate was cleaned with a piranha solution (3:1 (v/v) H_2SO_4:H_2O_2) at 120 °C for more than 20 min and followed by ultrasonication in deionized (DI) water for 10 min before use in experiments. The SLMs were formed on the prepared substrate by adsorption and rupture of the SUVs for more than 30 min at room temperature. Excess vesicles were removed by DI water replacing the vesicle suspension. The epifluorescence microscopy (Eclipse E600-POL, Nikon) was used in the Texas red channel for imaging the SLMs.

3. Preparation of the RBCs. For preparation of the RBCs, human blood was obtained from healthy male donors (18−28 years old) using a vacutainer with acid citrate dextrose and a 21-gauge needle (Becton Dickinson) on the day of each experiment. Platelet-rich plasma and buffy coat were removed by aspiration after centrifugation at 200 g for 15 min. The centrifuged RBCs were washed three times with phosphate buffered saline (1 mM KH_2PO_4, 154 mM NaCl, 3 mM Na_2HPO_4, pH 7.4) and once with Tris buffer (15 mM Tris−HCl, 150 mM NaCl, 5 mM KCl, 2 mM $MgCl_2$, pH 7.4). The washed RBCs were resuspended in Tris buffer and deposited on the SLM-coated substrates by gravitational sedimentation at the concentration of 10^7 cells/mL for 30 min. The RBC-attached substrate was then held upside down for more than an hour in Tris buffer until the RBCs were detached from the porous regions by the gravitational force.

Results and Discussion

We first discuss the theoretical criterion for adhesion of the SLM on the porous region from the framework of the curvature elasticity. According to de Gennes's description of fluctuations in smectic liquid crystals,[18] the Helfrich-type bending energy per unit area of a fluid membrane is written as[19,21] $f = (K/2)(k_1 + k_2)$,[2] where the spontaneous curvature of the SLMs was assumed to be zero. Here, K denotes the bending modulus of the membrane, and k_1 and k_2 are two principle curvatures of the porous surface. Assuming that the pore is simply a hemisphere whose radius is r (Figure 3a), both k_1 and k_2 are then equal to $1/r$. In our case, the pore radius is typically on

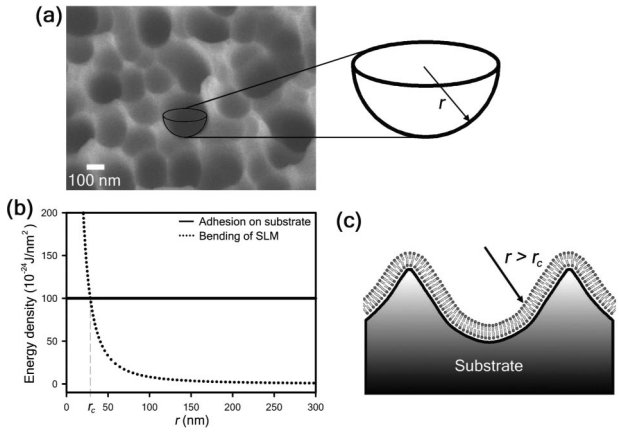

Figure 3. Adhesion criterion for the SLM on the porous topography: (a) the SEM image of pores and a hemisphere with a radius of r representing a pore; (b) the energy densities of adhesion and bending of the SLM as a function of r; (c) a schematic diagram of the SLM that follows the pore surface for $r > r_c$.

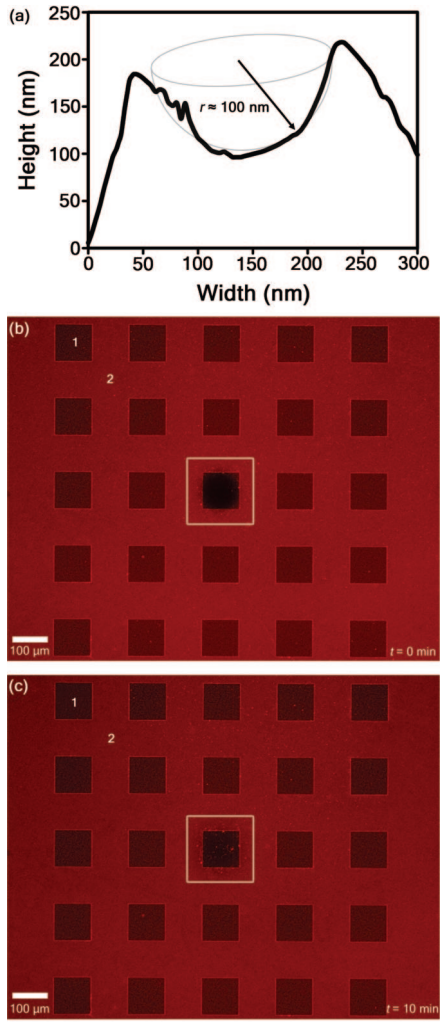

Figure 4. Profile of a pore and the formation of the SLMs on the flat and porous regions: (a) the AFM profile of a pore and epifluorescence micrographs of the FRAP on the SLM at (b) $t = 0$ min and (c) $t = 10$ min showing the 2-D fluidity as well as the continuity.

the order of 100 nm, as shown in Figure 3a. With the literature value of the adhesion energy per unit area[22] of the SLM on a glass substrate, 10^{-22} J/nm^2, and that of the bending modulus[23] of the SLM, 10 k_BT, the energy densities for adhesion and bending of the SLM on the porous surface are given as a function of r, as shown in Figure 3b. As shown in Figure 3b, the adhesion energy becomes larger than the bending energy above a certain critical radius, $r_c \approx 30$ nm. For $r > r_c$, the SLM prefers to be adsorbed on the porous surface and to follow the pore morphology in a conformal fashion, as shown in Figure 3c.

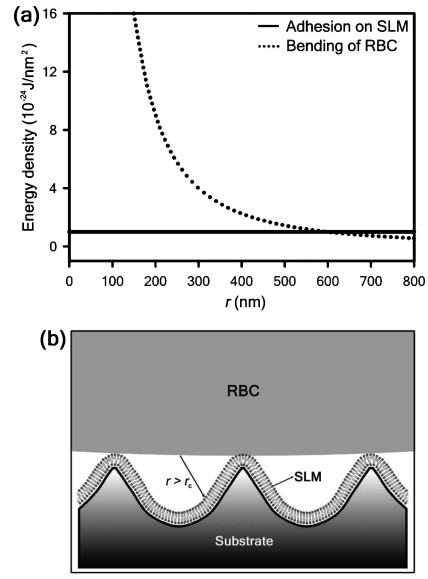

Figure 5. Adhesion criterion for the RBC on the SLM: (a) the energy densities of adhesion and membrane bending of the RBC; (b) a schematic diagram of the RBC on the SLM in the porous region.

Figure 4a shows a cross-sectional profile of a typical pore, measured with an atomic force microscope (AFM; SPA 400, Seiko Instruments), in the porous region. It represents indeed a hemispherical shape of a pore. The radius of the pore is about 100 nm which is more than 3 times larger than r_c. As a consequence, it is expected that the SLM covers continuously the porous region, satisfying $r > r_c$ in addition to the flat region ($r = \infty$). Figure 4b and c shows epifluorescence micrographs of the SLMs that were formed on the substrate with a 2-D array of the flat regions (label "1" in Figure 4b and c) in the porous background (label "2" in Figure 4b and c). From the contrast of the red fluorescence between region 1 and region 2, the population of the Texas red-DHPE molecules is rich in region 2 because of the large surface area in the porous region. This indicates that the SLM followed well the porous topography ($r > r_c$) as predicted above. Another important issue of the SLM as a biomimetic system is that 2-D fluidity and continuity should be maintained on the pore surface. As a direct assessment, the fluorescence recovery after photobleaching (FRAP)[24] study was carried out on the Texas red-DHPE molecules in a flat region (Figure 4b). The FRAP study shows that the photobleached area in region 1 (a black area enclosed by a white rectangle) was completely recovered after 10 min (Figure 4c) due to the free diffusion of lipid molecules from the background (region 2). The FRAP results confirm that both region 1 and region 2 were fully covered with the SLM having the fluidity.

Let us now describe how adhesion of the RBCs on the SLM is selectively produced, i.e., only in the flat regions. As in the case of the SLM, adhesion of the RBC will be governed by the competition between the strength of surface adhesion and the bending elasticity of the plasma membrane of the RBC. Figure 5a shows the energy densities for adhesion and bending of the plasma membrane of the RBC on the SLM as a function of r. For the RBC case, the adhesion energy per unit area[16] of $W_{RBC} = 10^{-24}$ J/nm^2 on a SLM and the bending modulus[15] of

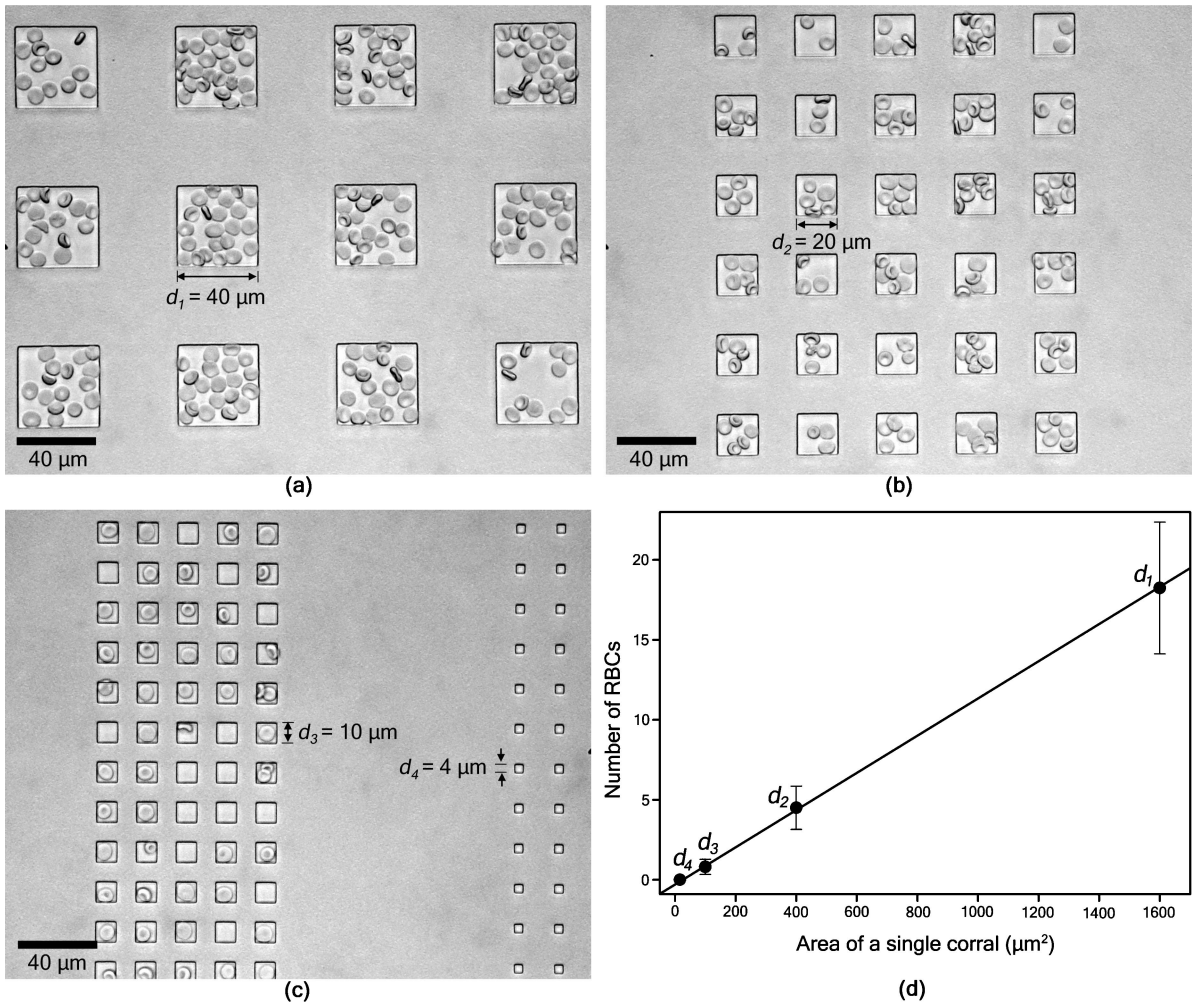

Figure 6. Microscopic images of the RBC arrays. Selective adhesion of the RBCs to the flat regions with the dimensions of (a) $d_1 = 40\ \mu$m, (b) $d_2 = 20\ \mu$m, and (c) $d_3 = 10\ \mu$m together with $d_4 = 4\ \mu$m, and (d) the population of the RBCs in a single corral in the microarray.

$K_{RBC} = 44\ k_BT$ were used in the calculations. In contrast to the SLM, for pores with $r \approx 100$ nm, the bending energy of the RBC membrane is much higher than the adhesion energy. As a result, adhesion of the RBCs will be energetically favorable only in the flat regions ($r = \infty$) but not in the porous regions. This can be seen clearly in Figure 5b. Ideally, for the pore radius greater than the order of the physical dimension of the RBC (7−8 μm), the adhesion of the RBC on the SLM will be easily promoted in the porous region without elastic distortions. In a simple approximation, the adhesion of the RBC will be possible when $r > (2\ K_{RBC}/W_{RBC})^{1/2} \approx 600$ nm to 2 μm, depending on W_{RBC} in the range from 10^{-24} to 10^{-25} J/nm^2 (Figure 5a). In this case, the RBC will experience a certain amount of elastic distortions.

On the basis of the predictions made above, the site-selective adhesion of the RBCs in the flat regions was demonstrated in several RBC microarrays. Parts a−c of Figure 6 show microscopic images of the RBC arrays whose dimensions of the flat regions are $d_1 = 40\ \mu$m, $d_2 = 20\ \mu$m, and $d_3 = 10\ \mu$m together with $d_4 = 4\ \mu$m, respectively. As predicted, the RBCs were completely confined within the flat corrals and detached from the background porous regions. The number of the RBCs confined in each corral was dictated by the physical dimension of the flat corral. Especially in the case of $d_3 = 10\ \mu$m that is comparable to the lateral size of the RBC ($s = 7-8\ \mu$m), only a single RBC was contained in a corral, as shown in Figure 6c. For an extreme case of $d_4 = 4\ \mu\text{m} < s$, no RBC is confined inside a corral. This suggests that the adhesion energy W_{RBC} is on the order of 10^{-25} J/nm^2, giving the critical pore radius of a few microns, which is consistent with our first-order approximation discussed above. The population of the RBCs as a function of the corral dimension is plotted in Figure 6d. As the corral area increases, the number of the RBCs increases linearly. From the linearity observed in Figure 6d, it was found that the average packing ratio of the RBCs in a corral (about 0.5) is well conserved in each microarray.

Conclusions

The site-selective adhesion of the RBCs on lipid membranes supported on patterned porous substrates was described within the framework of the curvature elasticity of a fluid membrane. It was found that one of the key parameters governing the formation of the SLMs and/or the adhesion of the RBCs is the pore radius relative to the curvature radius which represents the curvature elasticity of a membrane system. On the basis of the concept of elasticity-based patterning, a microarray of the RBCs was built up as a robust platform for studying cellular activities and for devising ultrasensitive cell-based biosensors. For other kinds of cells, the interplay between the adhesion and the geometrical curvature in two topographies needs to be precisely tuned to take account of the forms and compositions of cell membranes. Finally, our topographic approach would be useful for fabricating a variety of membrane-associated

bioarrays where membrane−membrane interactions are site-selectively controlled through the elasticity on the SLMs.

Acknowledgment. We would like to thank J.-Y. Noh for the preparation of the RBCs and technical discussions. This work was supported in part by Zema International and Jein Medical Center, Korea.

References and Notes

(1) Barrett, E. W.; Phelps, M. V. B.; Silva, R. J.; Gaumond, R. P.; Allcock, H. R. *Biomacromolecules* **2005**, *6*, 1689.
(2) Nakanishi, J.; Kikuchi, Y.; Inoue, S.; Yamaguchi, K.; Takarada, T.; Maeda, M. *J. Am. Chem. Soc.* **2007**, *129*, 6694.
(3) Groves, J. T.; Mahal, L. K.; Bertozzi, C. R. *Langmuir* **2001**, *17*, 5129.
(4) Rider, T. H.; Petrovick, M. S.; Nargi, F. E.; Harper, J. D.; Schwoebel, E. D.; Mathews, R. H.; Blanchard, D. J.; Bortolin, L. T.; Young, A. M.; Chen, J. Z.; Hollis, M. A. *Science* **2003**, *301*, 213.
(5) Peppas, N. A.; Hilt, J. Z.; Khademhosseini, A.; Langer, R. *Adv. Mater.* **2006**, *18*, 1345.
(6) Lin, R.-Z.; Ho, C.-T.; Liu, C.-H.; Chang, H.-Y. *Biotechnol. J.* **2006**, *1*, 949.
(7) Revzin, A.; Tompkins, R. G.; Toner, M. *Langmuir* **2003**, *19*, 9855.
(8) Patrito, N.; McCague, C.; Norton, P. R.; Petersen, N. O. *Langmuir* **2007**, *23*, 715.
(9) Nishizawa, M.; Takoh, K.; Matsue, T. *Langmuir* **2002**, *18*, 3645.
(10) Falconnet, D.; Koenig, A.; Assi, T.; Textor, M. *Adv. Funct. Mater.* **2004**, *14*, 749.
(11) Tourovskaia, A.; Barber, T.; Wickes, B. T.; Hirdes, D.; Grin, B.; Castner, D. G.; Healy, K. E.; Folch, A. *Langmuir* **2003**, *19*, 4754.
(12) Ostuni, E.; Chapman, R. G.; Liang, M. N.; Meluleni, G.; Pier, G.; Ingber, D. E.; Whitesides, G. M. *Langmuir* **2007**, *17*, 6336.
(13) Falconnet, D.; Csucs, G.; Grandin, H. M.; Textor, M. *Biomaterials* **2006**, *27*, 3044.
(14) Yawata, Y. *Cell Membrane: The Red Blood Cell as a Model*; Wiley-VCH Verlag: Weinheim, Germany, 2003.
(15) Evans, E. A. *Biophys. J.* **1983**, *43*, 27.
(16) The adhesion energy between the plasma membrane of the RBC and the SLM was obtained from the experimental results of intermembrane adhesion of the RBCs: Evans, E. A. *Biophys. J.* **1980**, *30*, 265.
(17) Closse, C.; Dachary-Prigent, J.; Boisseau, M. R. *Br. J. Hamaetol.* **1999**, *107*, 300.
(18) de Gennes, P. G. *J. Phys. (Paris)* **1969**, *4*, C4–65, Colloque.
(19) Helfrich, W. *Z. Naturforsch. C* **1973**, *28*, 693.
(20) Buboltz, J. T.; Feigenson, G. W. *Biochim. Biophys. Acta* **1999**, *1417*, 232.
(21) For a comprehensive discussion, see: Safran, S. A. *Statistical Thermodynamics of Surfaces, Interfaces, and Membranes*; Addison-Wesley: New York, 1994; Chapter 6.
(22) Schonherr, H.; Johnson, J. M.; Lenz, P.; Frank, C. W.; Boxer, S. G. *Langmuir* **2004**, *20*, 11600.
(23) Chen, Z.; Rand, R. P. *Biophys. J.* **1997**, *73*, 267.
(24) Axelrod, D.; Koppel, D. E.; Schlessinger, J.; Elson, E.; Webb, W. W. *Biophys. J.* **1976**, *16*, 1055.

JP806753F